

Part I

CARBON FIBERS

FORMATION OF MICROSTRUCTURE IN MESOPHASE CARBON FIBERS

J. L. White[†], B. Fathollahi, and X. Bourrat

1 Introduction

Mesophase carbon fiber was invented in the 1970s, independently and simultaneously, from our viewpoint today, by Leonard Singer in the US (Singer, 1978) and by Sugio Otani in Japan (Otani, 1981). Both based their concepts on the role of the liquid-crystalline carbonaceous mesophase described by Brooks and Taylor in 1965. Both recognized two key steps: flow of the anisotropic liquid in the shear-stress field of the spinneret to align the disk-like molecules, and oxidation thermosetting to stabilize the shape and microstructure of the fiber prior to carbonization.

These inventions led to high expectations in the carbon materials community for the rapid attainment of fiber with superior properties at the low costs anticipated for a pitch product. Vigorous research activities ensued, many under conditions of proprietary secrecy. An important advance, with potential for many carbon materials besides fiber, was the development of more satisfactory mesophase pitches, fully transformed to the liquid-crystalline state and of low viscosity (Lewis and Nazem, 1987; Mochida *et al.*, 1988; Sakanishi *et al.*, 1992).

However for mesophase carbon fiber, the results fell short of expectations. The mechanical properties were not competitive with PAN-based fiber, except for some high-modulus grades. Low costs were never achieved, apparently due to the lengthy process of stabilization and the early 1990's saw downsizing and abandonment of research programs, with only a few products commercialized.

Nevertheless the prospects for a carbon fiber spun in the liquid-crystalline state continued to fascinate carbon scientists. Comprehensive microstructural studies initiated by Hamada *et al.* in 1987 demonstrated the remarkable flow memory of viscous mesophase in a simple spinneret. Then Bourrat *et al.* (1990a–c) showed that the nanostructure of as-spun filaments can be described in terms of the basic microstructural features of liquid crystals: bend, fold, splay, and disclinations.

Some practical results of manipulating the flow of mesophase in the spinneret became apparent. In a 1990 patent, Hara *et al.* showed that a fine-weave screen placed across the mesophase stream flowing to the spinneret can profoundly alter the microstructure of as-spun fiber. In 1993, Taylor and Cross reported their study of screened flow prior to spinning; their observations were rationalized in terms of an array of fine mesophase cylinders, leading directly to the concept of a filament comprised of a linear composite of near-nanotubes. Then rheologists entered the scene to study the flow instabilities of a discotic liquid crystal under the flow conditions in a spinneret (Singh and Rey, 1995, 1998; Didwania *et al.*, 1998), thus providing basic guidance for spinning experiments.

[†]In memorial of Jack White deceased in 2002.

Thus the stage is being set for a new class of mesophase carbon fibers, with designed microstructures produced by manipulating flow of the anisotropic liquid in the spinneret.

2 Microstructural approach

Consider first the microstructure of manufactured mesophase carbon fiber, keeping in mind that such fiber has been processed through stabilization, carbonization, and graphitization after spinning of the viscous mesophase. “Nanostructure” may seem more suitable to describe the architecture of graphitic layers in a filament whose diameter is near ten microns. The scanning electron micrograph (SEM) of Fig. 1.1 offers an example of fibers

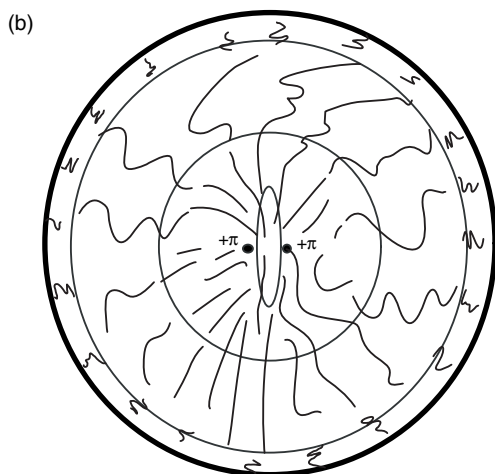
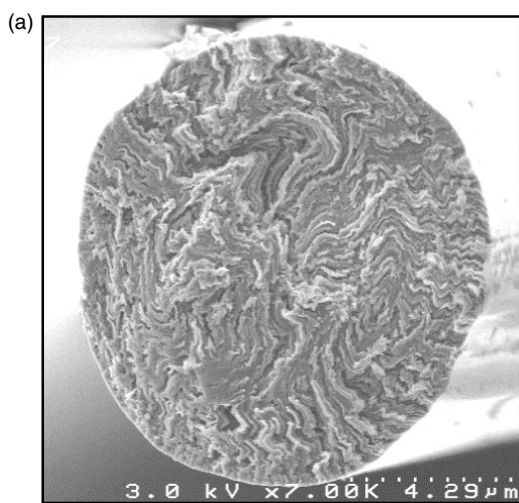


Figure 1.1 Fracture surface of a mesophase carbon filament (a) manufactured by DuPont (E35). The schematic diagram (b) outlines an oriented core bounded on each side by a $+\pi$ super-disclination and with wavy and rippled layers leading from the core to zigzag bands at the rim. From Bourrat (2000).

available in the 1980s. Such fibers, manufactured by Union Carbide and by DuPont, were studied extensively by Fitzgerald, Pennock, and Taylor (1991, 1993). Although there is some variability in structural detail, even in filaments from the same tow, the sketch outlines transverse features that are generic to most mesophase carbon fibers. This filament exhibits an oriented core with the surrounding layers in radial orientation. As a function of increasing radius, three zones may be seen in which the radial layers waver, ripple, and corrugate increasingly to form zigzag bands near the rim. Finally there is a thin skin, finely structured and highly corrugated.

Figure 1.2 includes a transmission electron micrograph (TEM) of the same type of fiber. The diffraction contrast defines the oriented core as well as the $+\pi$ super-disclination that accommodates the parallel layers of the oriented core to the radial layers in the surrounding zone. The term “super-disclination” is used to distinguish a new disclination imposed on an oriented mesophase body or stream that already may carry many disclinations from its previous history of coalescence and flow. An example is the formation of $+2\pi$ super-disclinations by passage of mesophase pitch through a screen, described later in some detail.

The higher-magnification TEM micrographs of Fig. 1.3 define layer orientations within the bands located near the rim of a DuPont fiber, here again in the as-spun condition.

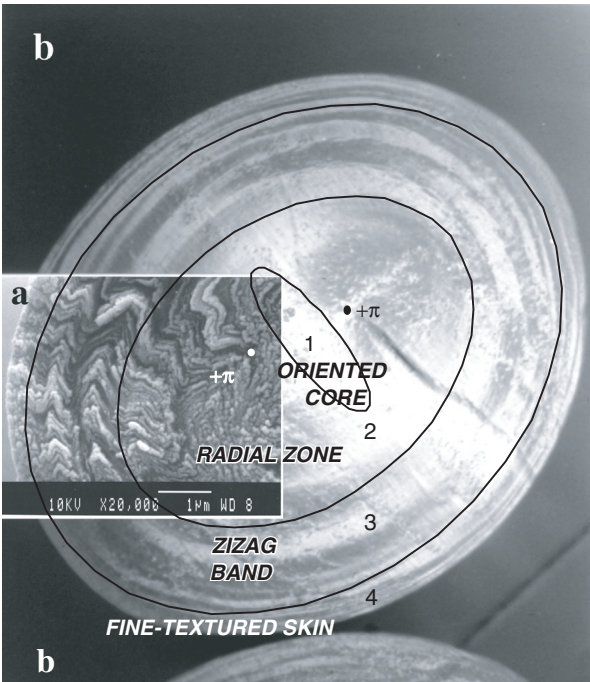


Figure 1.2 An SEM of a carbonized DuPont E35 filament superposed on a TEM dark-field image of the same type of fiber at the as-spun stage (a). The four zones observed in the carbonized filament are evident in the as-spun state (b). The elliptic shape is due to the angle of cutting of a circular filament. From Bourrat (2000).

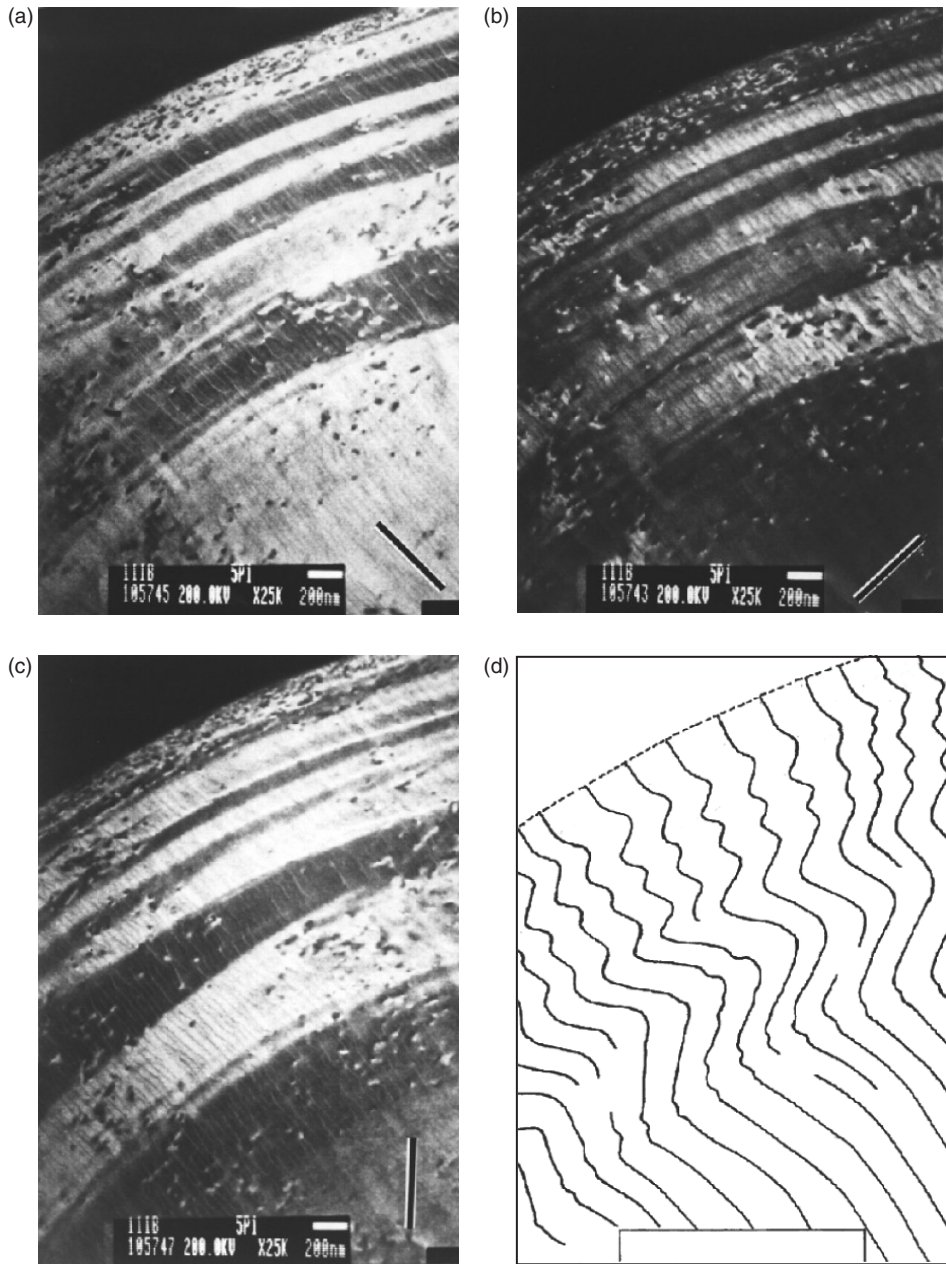


Figure 1.3 (a,b,c) Three TEM dark-field image at 45° rotation of diffraction vector show the zigzag bands in the rim of the Dupont filament in the as-spun condition. The bar in each micrograph defines the orientation of mesophase layers that appear bright. (d) Structural sketch illustrating the corrugated layer orientation.

The zigzag bands, only a fraction of a micron in width, consist of well-aligned layers within each band, and the boundaries are sharply defined. The zigzag angle, referred to later as the ripple angle, appears not to be fixed, but tends to 90° in the outer bands. Note the presence of many dots and short dashes appearing in reverse contrast to the bands in which they occur. These appear to be $+\pi/-\pi$ disclination loops (Zimmer and White, 1982) inherited from the mesophase pitch as it enters the spinneret; the contrast is due to the local rotation of mesophase molecules in the disclination loop. The density of dots is much higher in the skin, which may reflect the shear experienced briefly at the capillary wall as the stream exits the spinneret.

In 1990, Bourrat *et al.* (1990a) published observations by high-resolution electron microscopy (HREM) to identify $+\pi$ and $-\pi$ wedge disclinations on transverse sections of mesophase fiber heat-treated to 1600°C . Later these authors (Bourrat *et al.*, 1990b,c) demonstrated the presence of $+2\pi$ and -2π as well as $+\pi$ and $-\pi$ disclinations, along with bend, splay, and folding, in mesophase filaments in the as-spun condition. The presence of these liquid-crystalline structural features in finished fiber was confirmed by Pennock *et al.* (1993). Figure 1.4 is a lattice-fringe image of an Amoco P25 mesophase carbon filament (Bourrat *et al.*, 1990c); the structural diagram locates the $+\pi$, $-\pi$, and -2π disclinations in the micrograph. From these observations, mesophase carbon fibers may be viewed as carbonized fossils of highly oriented mesophase streams with non-equilibrium microstructures frozen in place as each stream is swiftly drawn to a filament.

Although an extensive patent literature has come to exist for mesophase carbon fiber, little information was published on the formation of microstructure within the spinneret until Hamada and co-workers at Nippon Steel undertook their comprehensive micrographic

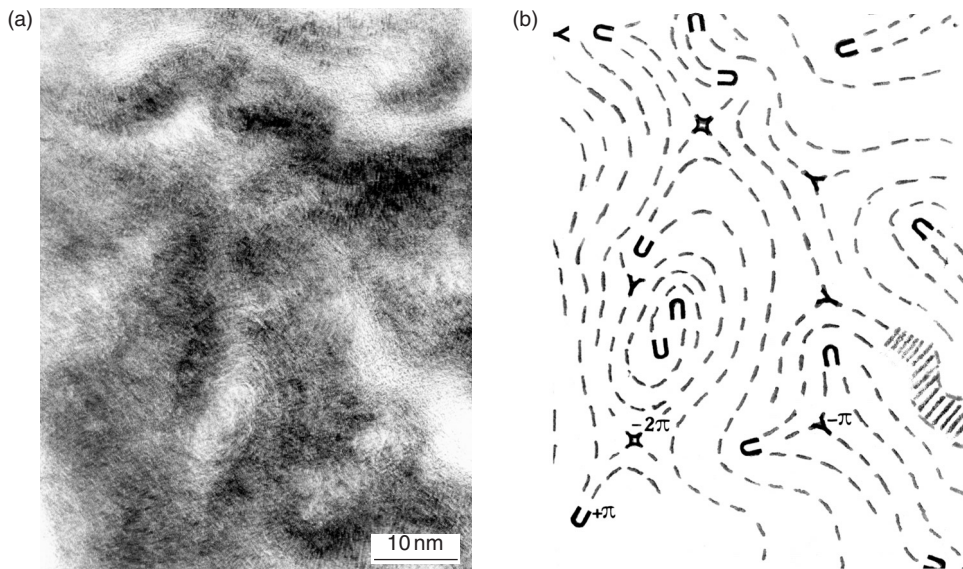


Figure 1.4 (a) A high resolution lattice-fringe of an Amoco P25 mesophase carbon filament. (b) The structure diagram locates $+\pi$ disclinations by U and $-\pi$ disclinations by Y. From Bourrat *et al.* (1990c).

studies, commencing with publication in 1987. The investigations included optical and electron micrography, as well as x-ray and electron diffraction, applied to monofilaments spun from a spinneret as outlined in Fig. 1.5a. The transverse microstructure, as-received from the pitch reservoir, or as modified by stirring before entrance to the capillary, was maintained with little loss of detail through extrusion and draw-down. The microstructural scale, as measured by the spacing of extinction contours, was found to be proportional to the diameter of the rod or filament, thus establishing the strong quantitative memory of viscous mesophase. When the stirrer was not in place, transverse sections of both extruded rods and spun filaments exhibited radial preferred orientation (PO), which was ascribed to convergent flow in the precapillary cone. Then the rapid extension and quench experienced in the draw-down cone were seen as critical factors in determining the final degree of radial orientation in the spun filaments (Hamada *et al.*, 1990).

Figure 1.5 illustrates schematically three types of monofilament spinnerets that have been used in exploring the formation of microstructure in mesophase fiber. Although some designs might be difficult to incorporate in an industrial multi-filament spinneret, their principal use at this point has been to demonstrate the wide range of microstructures that are accessible in spinning mesophase.

Figure 1.6 illustrates four such microstructures (Fathollahi, 1996) extruded from a low-viscosity mesophase pitch produced by alkylbenzene polymerization and pyrolysis (Sakanishi *et al.*, 1992). Figure 1.6a is a polarized-light micrograph of an extruded mesophase rod, at a stage just prior to draw-down to filament; in this case no special manipulation was applied to flow in the spinneret. The microstructure is that expected of a nematic liquid crystal, but the scale is very fine, e.g., disclinations can just be resolved. Sensitive-tint observations indicate a radial PO that strengthens with increasing radius. There are concentric markings in the rim (not shown here) that correspond in location to the zigzag bands of finished fiber.

In recent years rheologists have turned their attention to modeling the flow of a discotic nematic liquid crystal through a spinneret. The flow of an anisotropic liquid comprised of disk-like aromatic molecules was found to be inherently unstable, and rippled and zigzag structures are to be expected when the liquid enters a shear field (Didwania *et al.*, 1998; Singh and Rey, 1998). In 1D extension, the molecules will align with their largest dimension parallel to the extension, and 2D extension (as in the wall of an expanding bubble) will effect stronger alignment than 1D extension (Singh and Rey, 1995). The formation of $+2\pi$

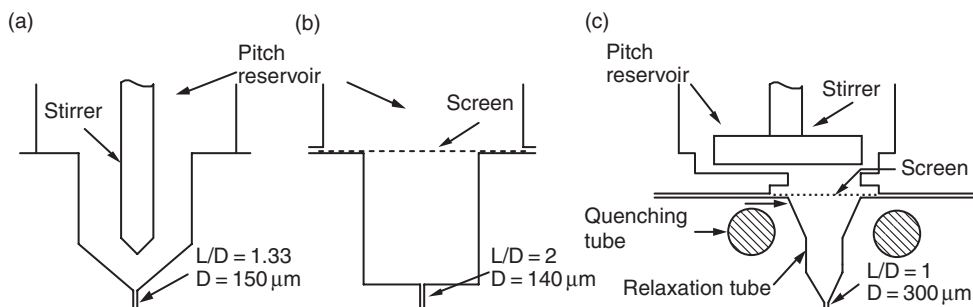


Figure 1.5 Schematic designs of three monofilament spinnerets used in laboratory-scale spinning: (a) stirring within the spinneret, from Hamada *et al.* (1988); (b) screened flow, from Matsumoto *et al.* (1993); (c) stirring with screened flow and quenching capability, from Fathollahi *et al.* (1999a).

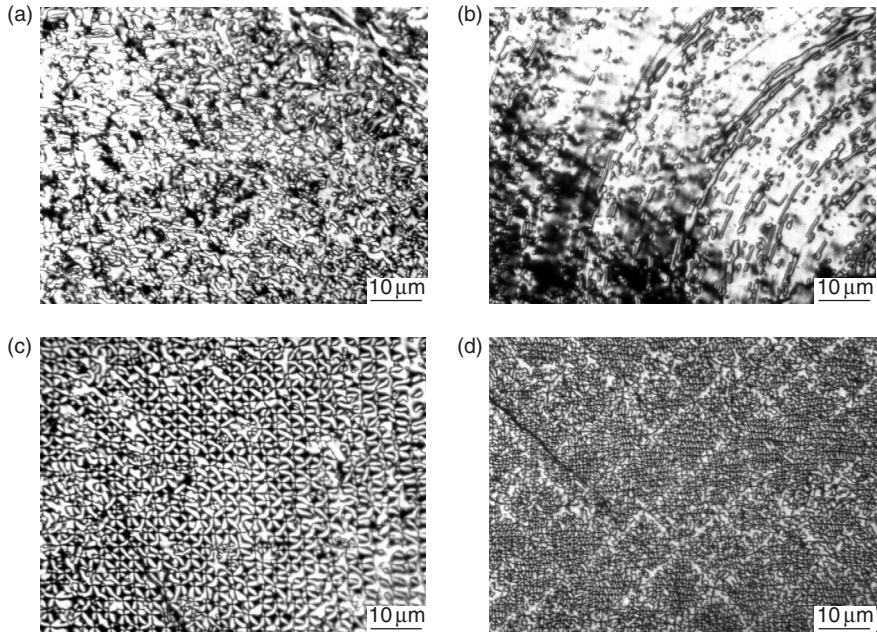


Figure 1.6 Some effects of manipulating mesophase flow within the spinneret, as observed on transverse sections of extruded rods: (a) direct flow from pitch reservoir without manipulation, some radial PO is present; (b) flow with strong stirring, concentric PO can be produced; (c) flow through a single 200-mesh screen, with some relaxation after passing the screen; (d) flow through two screens of 400- and 50-mesh, oriented at 45° each other. Crossed polarizers.

disclination arrays in screened flow (described later) has been modeled using Ericksen-Leslie continuum equations (Didwania *et al.*, 1999a). The analysis reveals a class of spatially periodic solutions to these equations for specific values of Leslie viscosities. An array of $+2\pi$ disclinations, oriented along the flow direction is observed in the regions of negligible shear in the transverse plane.

3 Manipulation of mesophase flow in a spinneret

Hamada's observations (1988) of the proportional reduction of microstructure by spinning lead directly to a concept of microstructural miniaturization, in which flow is manipulated to produce a desired microstructure at a workable scale in the upper part of the spinneret, then this is reduced by a thousand-fold to a nearly identical nanostructure by convergent flow in the capillary and draw-down to the filament.

Flow manipulation must be limited by the need for simple design because industrial spin-packs use multiple spinnerets to spin fiber tow with as many filaments as practical. Even simple stirring may be difficult if the stirrer must extend into each spinneret as in Fig. 1.5a. Spinneret design should also avoid 180° entry geometry, as in Fig. 1.5b, where the corners can create a vortex or weak secondary flow which can produce pyrolysis bubbles into the mainstream (Fathollahi, 1996). Some practical flow manipulations include the use of screens, perforated plates, or even just a single transverse bar or slot (Ross and Jennings, 1992). A

relaxation zone below the region of flow disruption may be useful to allow the decay of short-lived structures generated by flow instabilities (Didwania *et al.*, 1999b).

Stirring in the pitch reservoir may be desirable to maintain thermal and chemical homogeneity, but this can induce concentric PO in the feed to the spinneret. Stirring also refines the scale of fibrous or lamellar microstructures entering the spinneret (Hamada *et al.*, 1988). Strong concentric stirring at the spinneret entrance can introduce a concentric PO sufficient to outweigh the radial PO induced by convergent flow later in the spinneret, thus producing a concentric microstructure in the extruded rod (see Fig. 1.6b).

Wire screens are readily incorporated in a spinneret and, if the mesh is sufficiently fine, can profoundly alter the microstructure to the grid pattern seen in Fig. 1.6c. Fine screens may need support by a coarse screen to withstand the stress involved in spinning at high levels of viscosity; this can produce the grid-within-a-grid microstructure seen in Fig. 1.6d. Hara *et al.* (1990) appear to have been first to publish the use of screens to benefit the microstructure and properties of mesophase carbon fiber; their patent emphasizes the need for timely passage from screen to capillary in order to produce a clear reduced grid in the spun filament. The studies of screened flow by Matsumoto *et al.* (1993) confirm Hamada's rule that the scale of microstructure remains proportional to the diameter of the stream.

Taylor and Cross (1993) used optical and electron microscopy to examine screened-flow microstructures and found the orthogonal arrays outlined in Fig. 1.7, where the lighter lines represent traces of mesophase layers on the transverse section. Even in extruded rods, the extinction contours lie near the limit of optical resolution, but the $\sqrt{2}$ -effect sketched into the diagram is helpful in recognizing, on a microscope with rotating stage, the orthogonal array of mesophase cylinders, each of which comprises a concentric $+2\pi$ disclination. Thus the microstructures in Figs. 1.6c–d indicate potential precursors for filaments consisting of a composite of nanotubes.

Non-circular spinnerets have been used to produce particular shapes, such as ribbons, where the goal is not a particular transverse microstructure but highly oriented mesophase in convenient form for good thermal conductivity (Robinson and Edie, 1996; Edie, 1998; Lu *et al.*, 2000). Matsumoto *et al.* (1993) have shown how a square or rectangular spinneret can be used to modify screened flow to give elegant Moire-like patterns of extinction contours.

The regular array of $+2\pi$ and $-\pi$ disclinations shown in Fig. 1.8 was observed in the initial screened flow experiments (Fathollahi, 1996). The balanced array of disclinations was produced by gentle flow through a 200-mesh screen. The potential feasibility of such detailed control of microstructure in the spinneret motivated the studies described next.

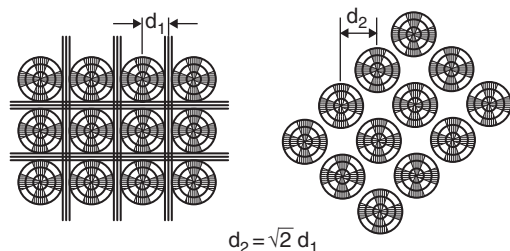


Figure 1.7 The orthogonal grid sketched by Taylor and Cross (1993) to represent the microstructure of a mesophase filament spun from a spinneret with a fine screen and observed on transverse section by crossed polarizers. On rotating the microscope stage by 45° , the spacing of extinction contours changes by $\sqrt{2}$ (Fathollahi, 1996).

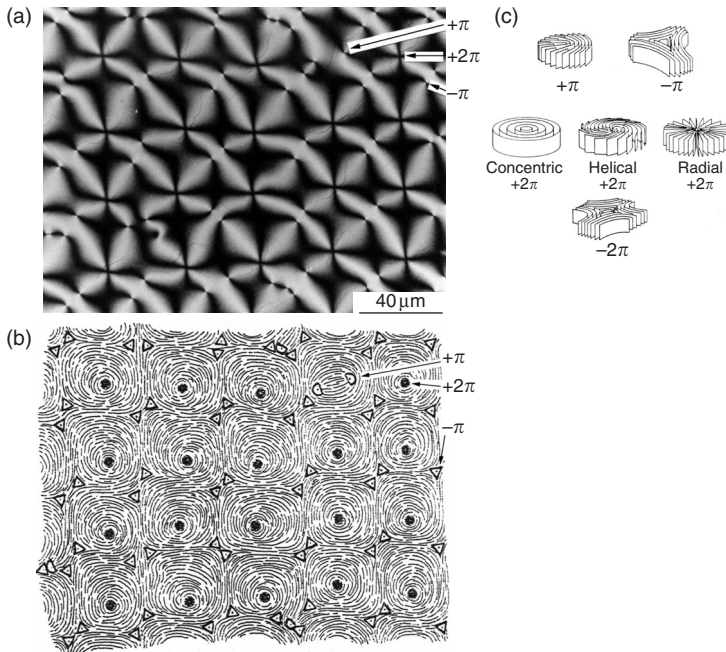


Figure 1.8 A regular array of wedge disclinations formed by mesophase after flow through a 200-mesh screen: (a) transverse section observed by crossed polarizers; (b) map of wedge disclinations defined by $\Delta = -\pi$, $D = +\pi$, $\bullet = +2\pi$; (c) wedge disclinations in a discotic liquid crystal (Zimmer and White, 1982). For a material in which the layers are parallel everywhere except at disclination cores, the total disclination strength over any appreciable field tends to zero.

3.1 Screened flow within the spinneret

Here we summarize studies at University of California at San Diego to understand how microstructure forms within a spinneret, utilizing stirring, screening, and relaxation to manipulate flow. Spinnerets of various designs were used; that shown in Fig. 1.5c is typical. All were machined from aluminum, for good thermal properties, and all incorporated quenching tubes to freeze structures in place when a desired spinning condition had been attained. Many spinnerets included one or two screens to establish cellular microstructures, and most included a relaxation tube to allow some decay of transient structures. The work described here used an alkylbenzene-based pitch (Sakanishi *et al.*, 1992), fully transformed to mesophase, and supplied by the Mitsubishi Oil Co. The softening point is 285 °C, and flow temperatures ranged from 290 to 315 °C, corresponding to a viscosity range of 325 to 20 Pa.s.

Upon passing through a plain square screen, a mesophase stream splits into a set of ministreams that rejoin below the screen to form an array of square cells (Fathollahi and White, 1994). Below each screen wire, a weld-zone forms, as seen in Fig. 1.9. The weld zone is narrow relative to the wire diameter, and initially the new and strongly oriented microstructure is finer than can be resolved by polarized light. The strong planar orientation in the weld zone result from 2D extension in passing the aperture (Singh and Rey, 1995). Mesophase more centrally located in each cell develops “ripples” in the shear fields of

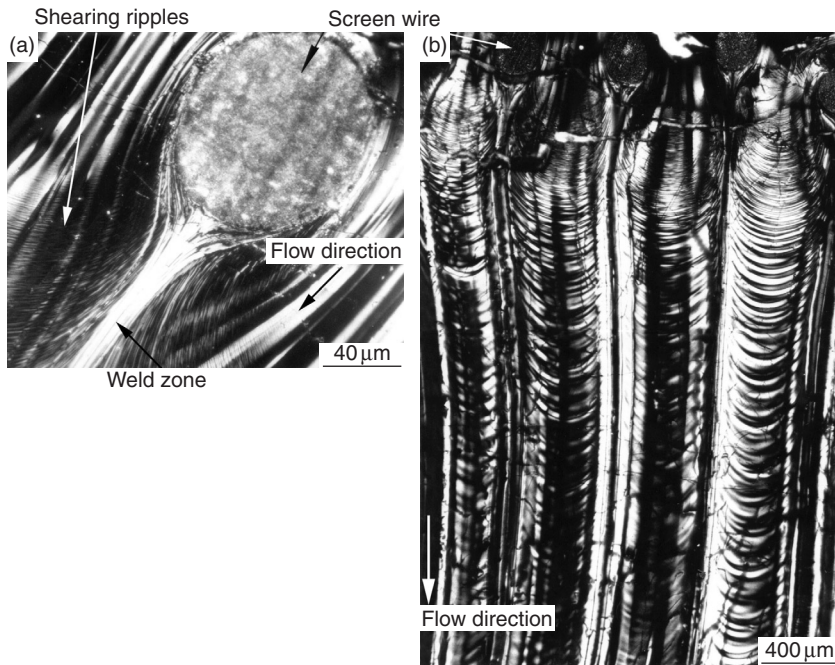


Figure 1.9 The passage of mesophase through a plain-weave screen. From Fathollahi (1996). (a) A highly oriented weld zone forms under the screen wire, and ripples appear in the shear field of the screen wire and (b) at lower magnification, the ripples are seen to decay soon after passage through the screen.

the wires. Although the ripples are extensive, they decay soon after the ministreams resume tubular flow, but substantial amounts of mesophase are left misoriented relative to the flow direction.

A transverse view at high-magnification of a mesophase stream immediately after penetrating a 100-mesh screen is given in Fig. 1.10a. The strong planar PO of the cell wall also appears on this transverse section, and the interior of the cell is intensely rippled in a concentric pattern everywhere but in the center. The same cell 330 microns below, or the equivalent of four seconds later, is illustrated in Fig. 1.10b. The cell walls have relaxed to lamellar microstructures that resemble the bubble walls found in needle coke (Zimmer and White, 1982). Within each cell, the ripples have coarsened and many have vanished, leaving a microstructure near that existing before passage through the screen.

If the foregoing experiment is conducted with a finer screen, e.g. 325 mesh, the cell walls tend to dominate the formation of new microstructure, as in Fig. 1.11. On this transverse section, relaxation has been sufficient for ripples to disappear, and most cells are dominated by a single $+2\pi$ super-disclination with a continuous core, indicated by the breadth of extinction at the core of each co-rotating cross. The cell walls have lost their strong lamellar PO, and their original locations are now defined by near-linear arrays of disclinations; in fact, the microstructure approaches that of the regular disclination array in Fig. 1.8.

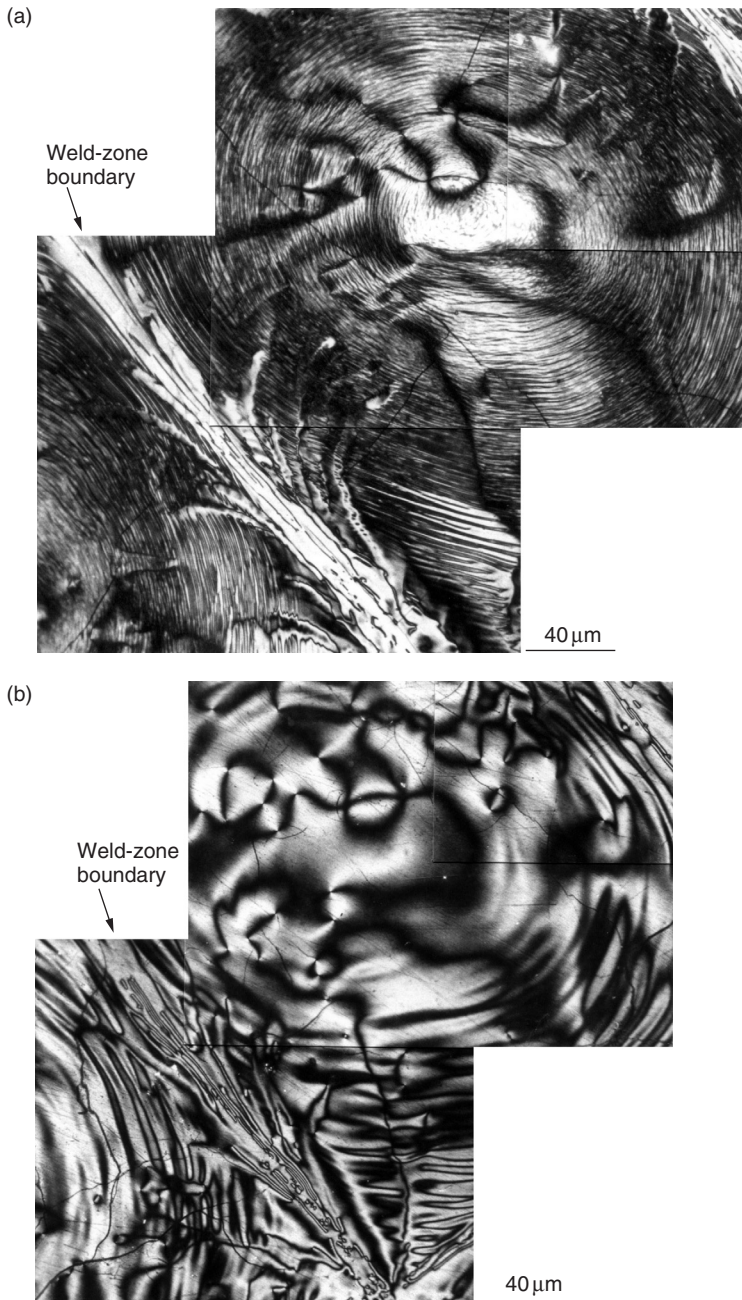


Figure 1.10 Transverse views of a mesophase ministream after passage through a 100-mesh screen: (a) immediately below screen and (b) 330 mm below section A. From Fathollahi (1996).

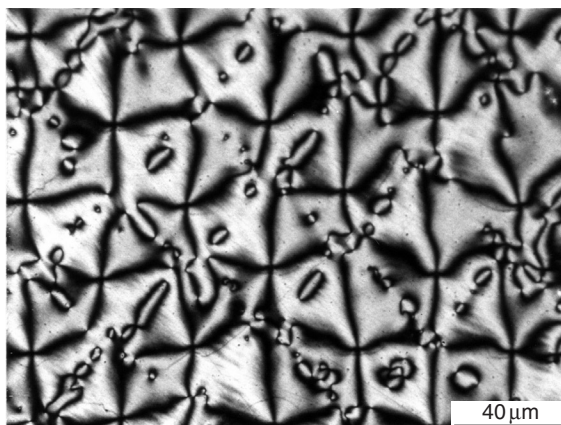


Figure 1.11 An array of $+2\pi$ disclinations formed after flow through a 325-mesh screen.

The observations of screen penetration confirm and add detail to the flow mechanism suggested by Taylor and Cross (1993), i.e. that flow over the wire of a square screen orients mesophase layers parallel to the wire. Thereafter two relaxation mechanisms operate with differing scales of relaxation time. The preferred orientations in cell walls and shear ripples decay rapidly. Disclination motions and reactions also occur, but much more slowly. Thus the weld zones, initially evident by strong lamellar PO, tend to be anchored by disclinations and are later located by the characteristic linear alignment of disclinations.

Passage through a screen directs flow along the spinneret axis (Fathollahi *et al.*, 1999a), but within each cell the mesophase can be seriously misoriented, as seen in Fig. 1.12a. Relaxation during tubular flow has little or no effect in reorienting layers within a cell, but when the stream enters a cone, convergent flow is strikingly effective, as seen in Figs. 1.12b and 1.12c. However some bright streaks do not disappear, and sensitive-tint observations find that most such streaks are blue on the right-hand side and orange on the left, indicating that the plane of section has intersected a cup-shaped structure similar to that sketched in Fig. 1.12e. Thus each bright streak corresponds to a $+2\pi$ disclination with the continuous core pointed downstream (Fathollahi *et al.*, 1996).

The transverse sections of Fig. 1.13 illustrate the effect of convergent flow in inducing radial PO in a mesophase stream. In this experiment, stirring in the reservoir produced some concentric PO that survived passage through the screen, as described for Fig. 1.13a. Sensitive-tint observations on extruded rod after convergent flow to the short capillary (Fig. 1.13b) indicate radial PO that increases in intensity with radius. This micrograph also displays fine concentric markings that cross the cell walls from the coarse screen; only the central core of the extruded rod is free of such markings. Figure 1.13c shows that the markings in some coarse cell walls fade or disappear upon rotation of the microscope stage.

The fine concentric markings were traced to their origin in the relaxation tube and were seen to be similar to ripples formed when mesophase penetrates a screen aperture (White *et al.*, 2001). Here the concentric geometry of the markings implies that they occur preferentially in radially oriented mesophase, i.e. when shear can act to wrinkle mesophase layers. Two observations at high magnification are offered in Fig. 1.14 to show that the

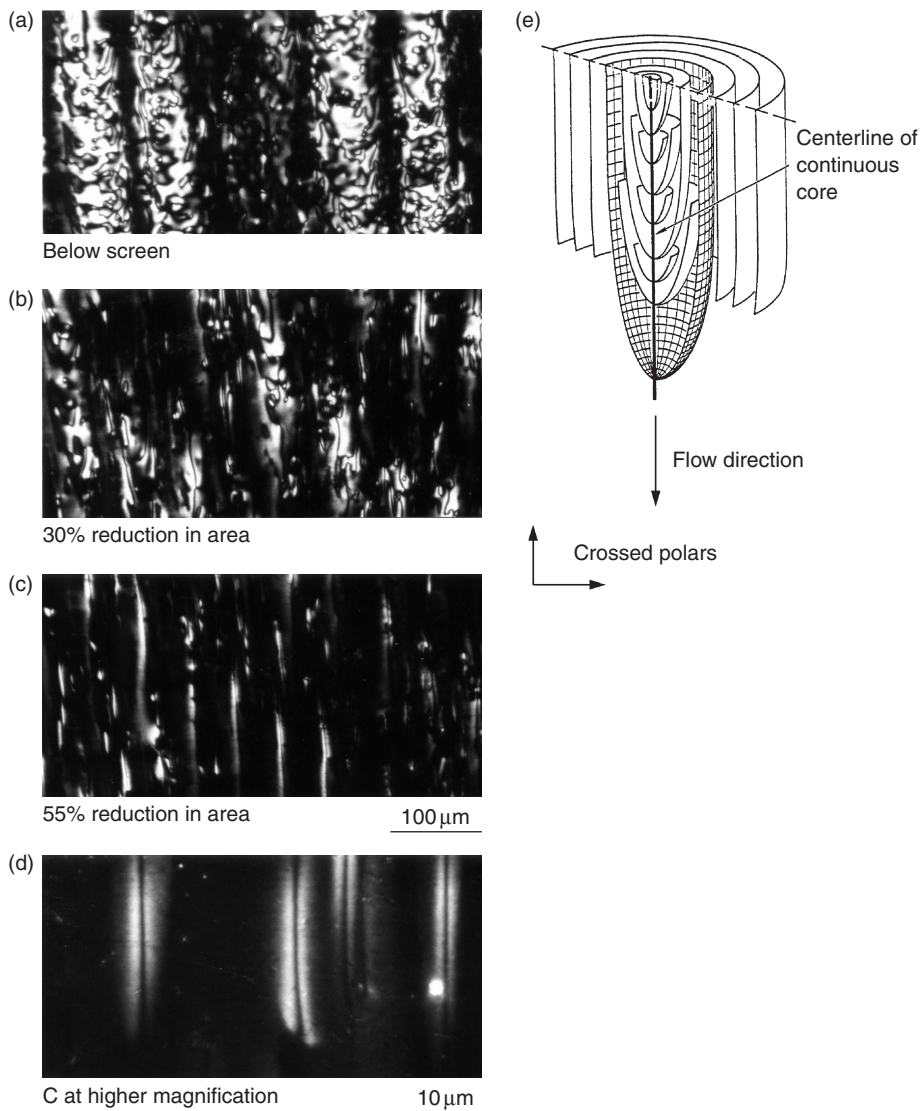


Figure 1.12 Longitudinal alignment of a screened stream by convergent flow in the entrance cone of a spinneret. From Fathollahi (1996). Polarizers oriented so that mesophase layers parallel to flow direction are dark. The bright streaks in (c) and (d) that are not eliminated by convergent flow correspond to cups of $+2\pi$ disclinations pointed in the flow direction, as sketched in (e).

markings vary in detail over the radius of the rod. [Figure 1.14a](#) illustrates blurred ripples that disappear upon stage rotation, while [Fig. 1.14b](#) shows more crisply defined bands that are common at high radius; the latter do not vanish upon stage rotation.

Measurements of the ripple angle R suggest the corrugated models of [Fig. 1.15](#); the ripple angle is not fixed, but tends to increase with radius. Near the rim, the ripple angle

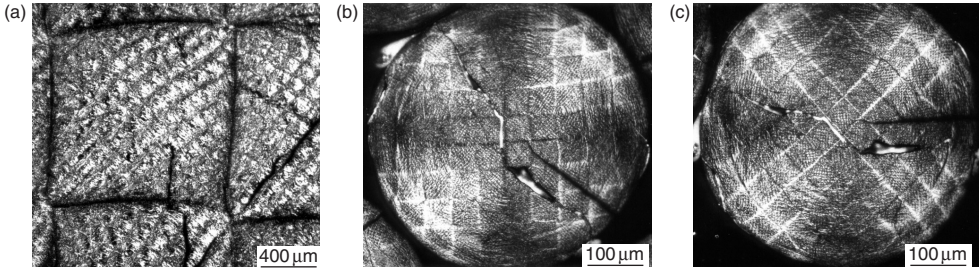


Figure 1.13 Convergent flow induces radial PO, as observed on transverse section below a screen: (a) in north-east quadrant of a stream just below screen, the sensitive-tint response is largely orange, indicating concentric PO; (b) for the same stream after convergent flow extruded rod, sensitive-tint response indicates radial PO that increases with radius; (c) same rod rotated by 45° , note that some concentric markings vanish upon rotation.

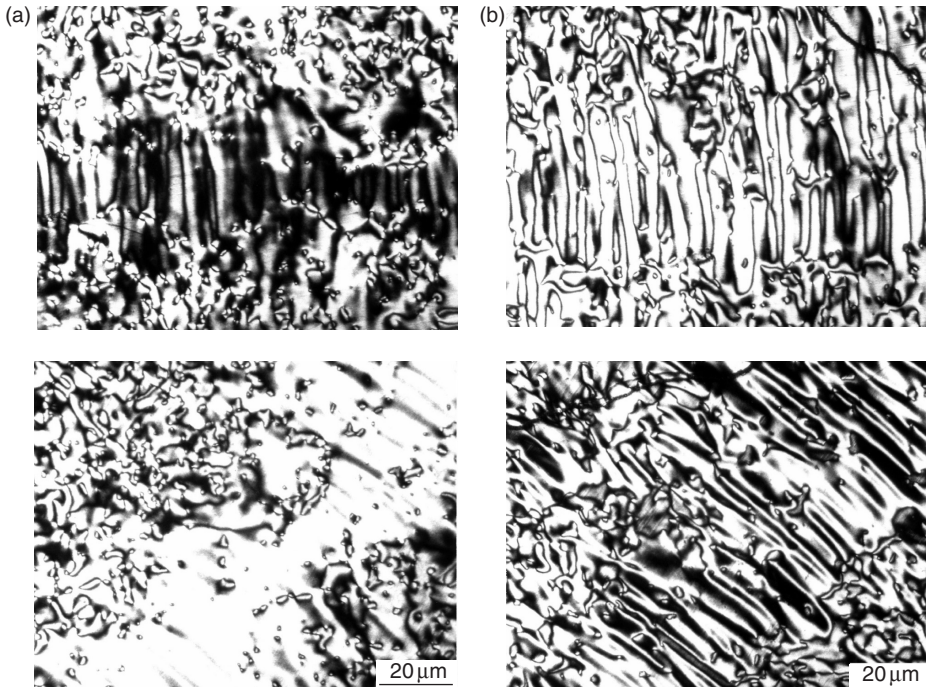


Figure 1.14 Two types of concentric ripples formed by shear of radially oriented mesophase in thick weld zone; the specimen was rotated 45° for the lower micrograph: (a) blurred ripples that disappear upon stage rotation and (b) crisply defined ripples that do not vanish upon stage rotation.

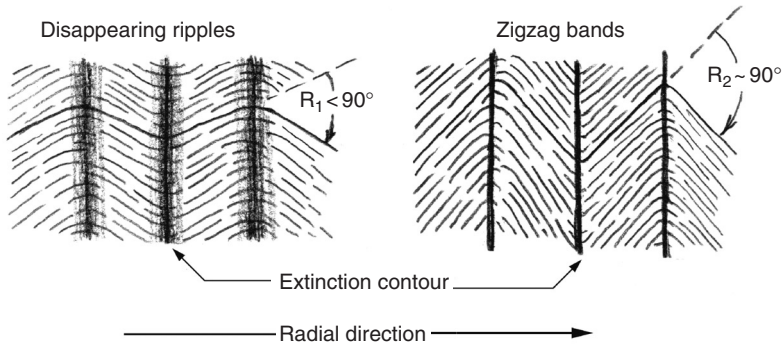


Figure 1.15 Schematic models, on transverse section, of ripples in radially oriented mesophase layers. If the ripples angle R is well under 90° , the ripples disappear upon rotation of the microscope stage.

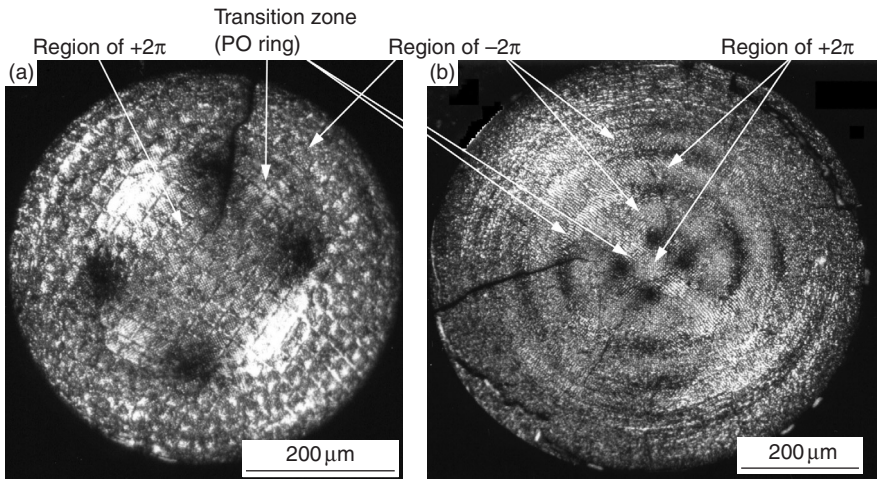


Figure 1.16 Preferred-orientation rings superposed on a screened grid by flow through a capillary: (a) rod extruded from a $457\ \mu\text{m}$ -diameter capillary with $L/D = 4$ and (b) rod extruded from a $710\ \text{mm}$ - diameter capillary with $L/D = 20$.

reaches 90° or higher, accounting for bands that do not fade upon stage rotation. Thus the ripples produced by shear acting on radially oriented mesophase appear to be precursors of both the wavy and zigzag microconstituents that are found in finished fiber.

3.2 Mesophase flow in capillary and draw-down cone

The linear flow rates in the capillary can limit further microstructural effects, since the residence time, even in a long capillary, is only a fraction of a second. McHugh and Edie (1995) have shown that the tendency to radial PO continues in the capillary. Two transverse effects

of flow in a long capillary are illustrated in Fig. 1.16 for streams that were screened and received some relaxation in the upper, slower-moving part of the spinneret. The radial PO appears in the form of rings that decrease in diameter and increase in number as the capillary is traversed (Fathollahi *et al.*, 1996). A thin banded layer, too fine in texture for optical resolution, appears at the rim and gradually grows in depth along the length of the capillary. Upon reaching the transition from shear to elongational flow at the capillary exit, this rim must accelerate more than the interior of the filament, leaving a thin, fine-textured outermost skin.

Mapping of the PO rings in the capillary finds each ring to consist of radially oriented mesophase sandwiched between regions of alternating arrays of $+2\pi$ and -2π disclinations, beginning with $+2\pi$ disclinations at the center (Fathollahi, 1996). Between the radially oriented rings, the disclination arrays retain their regularity of spacing, so the transition regions appear to be the scene of short-range reversible reactions between neighboring sets of disclinations; formally the reactions may be written as

$$(+2\pi) + 2(-\pi) = (-2\pi) + 2(+\pi)$$

Mesophase in the draw-down cone experiences rapid acceleration to spinning speed and sharp increases in viscosity as the filament cools. Despite the severe conditions, Fig. 1.16

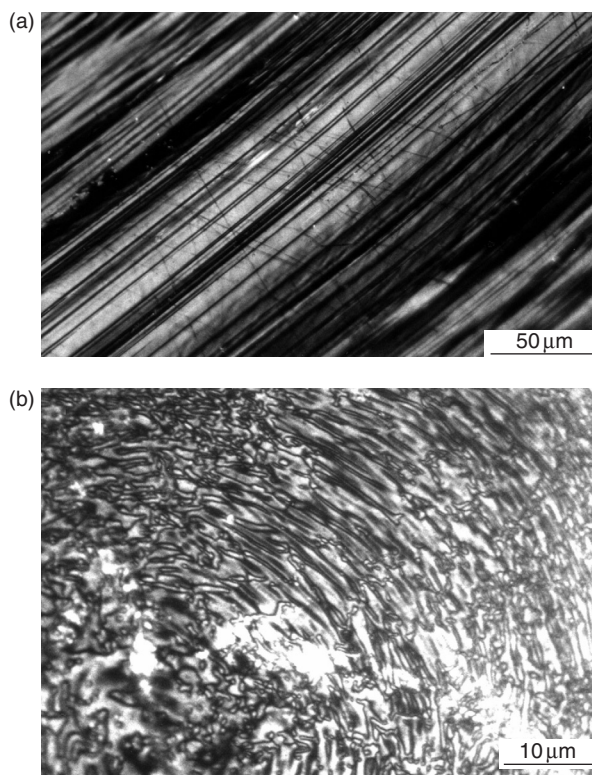


Figure 1.17 Draw-down cone quenched during spinning without a screen. (a) Longitudinal section, flow direction NE/SW and (b) transverse section. From Fathollahi (1996).

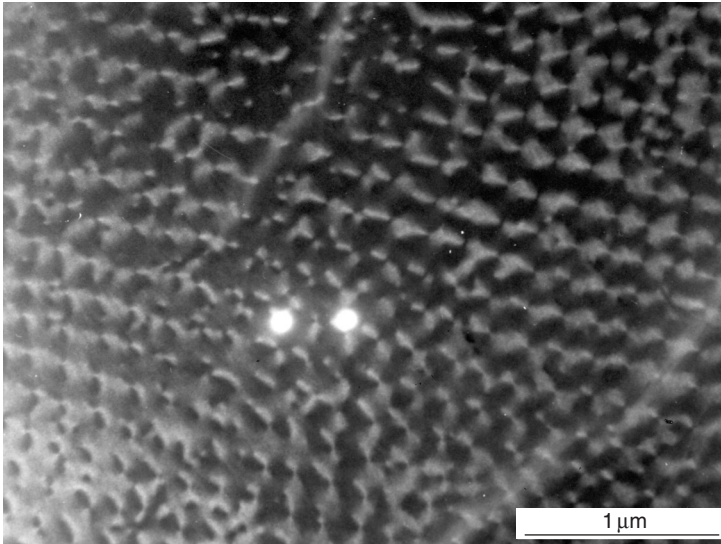


Figure 1.18 Dark-field electron micrograph at the core of an as-oxidized 30 μm filament. From Subramoney *et al.* (1996). The $+2\pi$ disclination are spaced at about 187 nm.

suggests that the processes of mesophase alignment and microstructural miniaturization run smoothly.

Figure 1.18, a dark-field electron micrograph of a filament spun with screened flow, shows that well-defined disclination arrays can be retained through spinning and stabilization with disclination spacings proportional to the filament diameter. This point has also been demonstrated for a grid-within-a-grid (Fathollahi *et al.*, 1997), for the $+2\pi$ and -2π disclination rings developed by flow through a capillary (Subramoney *et al.*, 1996; Fathollahi *et al.*, 1997), and for $+2\pi$ disclinations spaced as closely as 65 nm (Fathollahi *et al.*, 1999b).

3.3 Stabilization and heat treatment

To stabilize as-spun fiber against softening and loss of structure during carbonization, oxidation is practised at temperatures as high as 300 °C. However oxidation at such high temperatures appears to induce substantial carbon loss (Miura *et al.*, 1995) and reduced strength in the finished fiber (Yoon *et al.*, 1994). The potential for damage by carbon burnoff is most serious at the filament surface, since steeper oxygen gradients are required at higher oxidation temperatures to ensure stabilization to the center of the filament (Mochida *et al.*, 1989; Kasmer and Diefendorf, 1991).

Recent work indicates that oxidation can be conducted at temperatures as low as 130 °C, with substantial improvements to carbon yield and the depth of stabilization (Cornec *et al.*, 1992; Fathollahi *et al.*, 2000; Jones *et al.*, 2001). These benefits are thought to result from a reduced variety of active reaction sites on mesophase molecules at lower temperatures and thus less interference with oxygen diffusion. Although exposure times may be lengthy, the oxygen pressure can be increased to speed the process. Thus pressurized oxidation at low

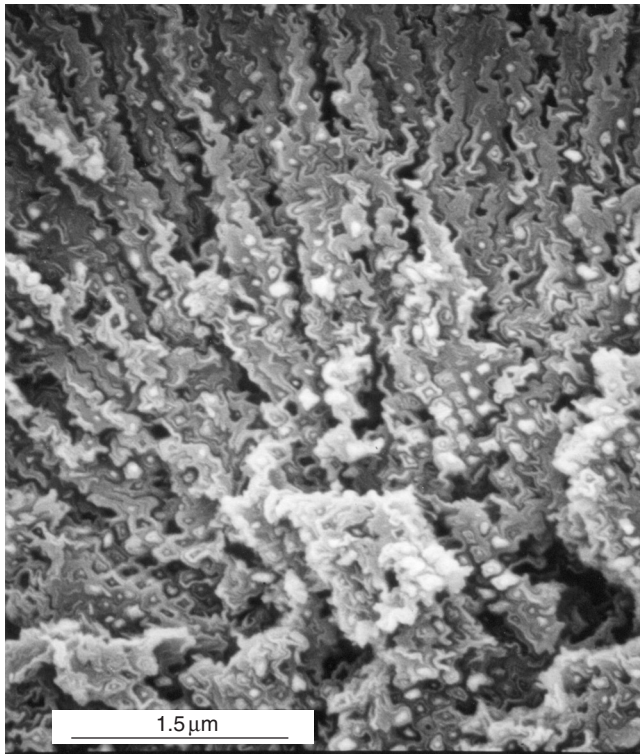


Figure 1.19 Shrinkage-cracking and $+2\pi$ disclination arrays in a screened filament that has been stabilized and heat-treated to $2,400^{\circ}\text{C}$. SEM of a filament fractured in tension. From Fathollahi *et al.* (1997).

temperature appears to offer stabilization with better oxygen distribution and less potential for damage by carbon burnoff near the fiber surface.

Figure 1.19 is a scanning electron micrograph of the fracture surface of a screened mesophase filament after stabilization and carbonization to $2,400^{\circ}\text{C}$ (Fathollahi *et al.*, 1997). The most obvious effects of carbonization are the wavering shrinkage cracks in the more radially oriented regions away from the core of the filament. Ordered arrays of white puffs, sometimes in small distorted boxes, appear most frequently near the core; these are believed to be $+2\pi$ disclination arrays because their spacing is proportionate to the filament diameter. Other types of disclinations are not readily identified in the highly serrated fracture surface, perhaps because $+\pi$ and $-\pi$ disclinations do not possess a structure like the cup-shaped core of the $+2\pi$ disclination shown in Fig. 1.12.

4 Discussion

The transverse microstructure sketched in Fig. 1.1 offers a useful framework to discuss mechanisms active in the spinning of mesophase fiber at viscosity levels where the structural memory is effective. The ripples, zigzag bands, and fine structure in the rim of the filament appear to be rheological consequences of the tendency for carbonaceous mesophase

to align radially during convergent and tubular flow in the spinneret (Didwania *et al.*, 1998; Singh and Rey, 1998).

To some extent, the thickness of outermost skin is open to control by spinneret design, such as the lengths of the relaxation and capillary tubes. Thus a major fraction of the filament within the skin will reflect a miniaturized microstructure of the mesophase entering the spinneret unless the filament designer elects to manipulate flow by such means as stirring, screens, and relaxation.

Plain-weave screens, at suitably fine mesh, can establish a completely new tubular microstructure, and the concept by Taylor and Cross (1993) of a composite filament consisting of a parallel array of graphene tubes, at a scale approaching that of a thick-walled buckytube, seems well worth pursuing. Their measurements of the mechanical properties on fibers only partially converted to nanotubular microstructures are promising, and the fiber user should be interested in such further developments as more fully nanotubular fibers, and in the mechanical toughness that might be contributed by adjusting capillary length to produce PO rings dominated alternately by $+2\pi$ and -2π disclinations.

The concept of producing nanotubular structures by screened spinning of mesophase pitch is intriguing. How far such a process can be driven to produce structures approximating thick-walled buckytubes seems to depend on the precision with which the layer-by-layer polymerization of mesophase molecules in a spun filament can be conducted through stabilization and carbonization to form graphene tubes or scrolls.

The process of low-temperature stabilization (Cornec *et al.*, 1992; Jones *et al.*, 2001) may play a role in improving fiber properties by offering better oxygen distribution at depth in the filament as well as less carbon burnoff at the surface. The practical objections of process length and increased cost may be relieved, at least in part, by using oxygen at pressures of the order of 1 MPa, but the immediate goal should be to learn if pressurized stabilization at low temperature offers a path to the high strengths that Bacon (1960) observed in carbon whiskers recovered from carbon deposits formed in high-pressure graphite arcs.

In closing, we are reminded that the present studies of what can be done to design and control the microstructure in spinning mesophase filaments was enabled by the development of low-viscosity, fully transformed mesophase pitches that are relatively stable at spinning temperatures. It is perhaps now reasonable to ask further help from aromatic organic chemists, to produce more ribbon-like than disk-like mesophase molecules with the length-to-width ratio of the molecules defined by rheological considerations, and to design only enough oxygen-reactive sites on the molecules to ensure stabilization with minimal carbon burn-off.

Acknowledgments

The authors are much indebted to Drs S. Subramoney and J. G. Lavin of the DuPont Experimental Station for their extensive electron microscopy; to B. D. Jones and Professor P. C. Chau for recent results on low-temperature stabilization; and to Dr A. K. Didwania for rheological insight. We also thank Professor G. H. Taylor (Australian National University) and Dr L. S. Singer (retired from Union Carbide) for valuable discussions. Mitsubishi Oil, Mitsubishi Gas Chemical, and Amoco Performance Products have been generous in providing mesophase pitches. This review, as well as the experimental work at UCSD, were supported by the US National Science Foundation under Grant No. 9700177.

References

- Bacon, R. (1960) "Growth, Structure, and Properties of Graphite Whiskers," *J. Applied Phys.*, **31**, 283–90.
- Bourrat, X. (2000) "Structure in Carbon and Carbon Artefacts," in *The Science of Carbon Materials*, H. Marsh and F. Rodriguez-Reinoso, Eds, Universidad de Alicante, Spain.
- Bourrat, X., E. J. Roche, and J. G. Lavin (1990a) "Lattice Imaging of Disclinations in Carbon Fiber," *Carbon*, **28**, 236–8.
- Bourrat, X., E. J. Roche, and J. G. Lavin (1990b) "Structure of Mesophase Pitch Fibers," *Carbon*, **28**, 435–46.
- Bourrat, X., E. J. Roche, and J. G. Lavin (1990c) "The Role of Disclinations in the Structure of Mesophase-Pitch-Based Carbon Fiber," Proc. International Symposium on Carbon, Tsukuba, Japan, 4–8 Nov. 1990, *Tanso publisher*, 790–3 and 320–2.
- Brooks, J. D. and G. H. Taylor (1965) "The Formation of Graphitizing Carbons from the Liquid Phase," *Carbon*, **3**, 185–93.
- Cornec, L. P., D. K. Rogers, C. C. Fain, and D. D. Edie (1992) "A Novel Stabilization Technique and its Influence upon Carbonization Yield," *Extended Abstracts, Carbon '92*, 710–12.
- Didwania, A. K., B. Fathollahi, and J. L. White (1998) "Formation of Banded Microstructure during Capillary Flow of Mesophase Pitch," *Extended Abstracts, Eurocarbon '98*, **2**, 531–2.
- Didwania, A. K., B. Fathollahi, and J. L. White (1999a) "Periodic Disclination Arrays in Carbonaceous Mesophase Pitch," *Extended Abstracts, Carbon '99*, 112–13.
- Didwania, A. K., B. Fathollahi, and J. L. White (1999b) "Capillary Flow of Carbonaceous Mesophase and its Stability," *Extended Abstracts, Carbon '99*, 482–3.
- Edie, D. D. (1998) "The Effect of Processing on the Structure and Properties of Carbon Fibers," *Carbon*, **36**, 345–62.
- Fathollahi, B. (1996) "Flow-Induced Microstructures in the Spinning of Carbonaceous Mesophase, a Discotic Nematic Liquid Crystal," PhD Thesis, University of California, San Diego.
- Fathollahi, B. and J. L. White (1994) "Polarized-Light Observations of Flow-Induced Microstructures in Mesophase Pitch," *J. Rheology*, **38**, 1591–607.
- Fathollahi, B., J. L. White, S. Subramoney, and J. G. Lavin (1996) "Designed Microstructures in Spinning Mesophase Pitch Fibers: Part I – Optical Microscopy," *Extended Abstracts, Carbon '96*, 200–1.
- Fathollahi, B., J. L. White, S. Subramoney, and J. G. Lavin (1997) "Designed Nanotubular Microstructures in Mesophase Carbon Fiber," in *Recent Advances in the Chemistry and Physics of Fullerenes and Related Materials*, **5**, K. M. Kadish and R. S. Ruoff, Eds, The Electrochemical Soc., Pennington, NJ, 538–48.
- Fathollahi, B., A. K. Didwania, and J. L. White (1999a) "The Formation of $+2\pi$ Disclination Arrays during Flow of Mesophase Pitch through a Screen Mesh," *Extended Abstracts, Carbon '99*, 362–3.
- Fathollahi, B., J. L. White, S. Subramoney, and J. G. Lavin (1999b) "Nanotubular Microstructures in As-Spun and Heat-Treated Mesophase Filaments," *Extended Abstracts, Carbon '99*, 486–7.
- Fathollahi, B., B. Jones, P. C. Chao, and J. L. White (2000) "Mesophase Stabilization at Low Temperatures," *Extended abstracts, Carbon '00* (Berlin, Germany), 259–60.
- Fitzgerald, J. D., G. M. Pennock, and G. H. Taylor (1991) "Domain Structure in Mesophase Pitch-Based Fibres," *Carbon*, **29**, 139–64.
- Hamada, T., T. Nishida, Y. Sajiki, and M. Matsumoto (1987) "Structure and Physical Properties of Carbon Fibers from Coal Tar Mesophase Pitch," *J. Mat. Res.*, **2**, 850–7.
- Hamada, T., T. Nishida, M. Furukama, and T. Tomioka (1988) "Transverse Structure of Pitch Fiber from Coal Tar Mesophase Pitch," *Carbon*, **26**, 837–41.
- Hamada, T., M. Furukama, Y. Sajiki, T. Tomioka, and M. Endo (1990) "Preferred Orientation of Pitch Precursor Fibers," *J. Mat. Res.*, **5**, 1271–80.
- Hara, R., M. Kagizaki, T. Takekura, and S. Tomono (1990) "Process for the Production of Pitch-Type Carbon Fibers," US Patent 4,923,648.

- Jones, B., B. Fathollahi, J. L. White, A. K. Didwania, and P. C. Chau (2001) "Mesophase Stabilization at Low Temperatures and Elevated Oxidation Pressures," *Extended Abstracts, Carbon '01*.
- Kazmer, A. J. and R. J. Diefendorf (1991) "Oxidative Stabilization of Bulk Carbonaceous Materials," *Extended Abstracts, 20th Conf. on Carbon*, 178–9.
- Lewis, I. C. and F. F. Nazem (1987) "Rheology of Mesophase Pitch – Effects of Chemical Constitution," *Extended Abstracts, 18th Conf. on Carbon*, 290–1.
- Lu, S., S. P. Appleyard, and B. Rand (2000) "Novel Highly Oriented Mesophase-Based Graphite (HOMG) for Thermal Management Applications," *Extended Abstracts, Eurocarbon 2000*, 236–7.
- Matsumoto, M., T. Iwashita, Y. Arai, and T. Tomioka (1993) "Effect of Spinning Conditions On Structures of Pitch-Based Carbon Fiber," *Carbon*, **31**, 715–20.
- Miura, K., H. Nakagawa, and K. Hashimoto (1995) "Examination of the Oxidative Stabilization Reaction of the Pitch-Based Carbon Fiber through Continuous Measurement of Oxygen Chemisorption and Gas Formation Rate," *Carbon*, **33**, 275–82.
- McHugh, J. J. and D. D. Edie (1995) "Orientation of Mesophase Pitch in Capillary and Channel Flows," *Liquid Crystals*, **18**, 327–35.
- Mochida, I., K. Shimizu, Y. Korai, H. Otsuka, and S. Fujiyama (1988) "Structure and Carbonization Properties of Pitches Produced Catalytically from Aromatic Hydrocarbons with HF/BF₃," *Carbon*, **26**, 843–52.
- Mochida, I., H. Toshima, Y. Korai, and T. Hino (1989) "Oxygen Distribution in Mesophase Pitch Fiber after Oxidation Stabilization," *J. Mat. Sci.*, **24**, 389–94.
- Otani, S. (1981) "Carbonaceous Mesophase and Carbon Fibers," *Mol. Cryst. Liq. Cryst.*, **63**, 249–64.
- Pennock, G. M., G. H. Taylor, and J. D. Fitzgerald (1993) "Microstructure in a Series of Mesophase Pitch-Based Fibers from DuPont: Zones, Folds, and Disclinations," *Carbon*, **31**, 591–609.
- Robinson, K. E. and D. D. Edie (1996) "Microstructure and Texture of Pitch-Based Ribbon Fibers for Thermal Management," *Carbon*, **34**, 13–36.
- Ross, R. A. and U. D. Jennings (1992) "Method of Making Small Diameter High Strength Carbon Fibers," US Patent 5,169,584 (December 8, 1992).
- Sakanishi, A., Y. Korai, I. Mochida, K. Yanagida, M. Noda, I. Thunori, and K. Tate (1992) "Comparative Study of Isotropic and Mesophase Pitches Derived from C₉ Alkylbenzenes," *Carbon*, **30**, 459–66.
- Singer, L. S. (1978) "The Mesophase and High-Modulus Carbon Fibers from Pitch," *Carbon*, **16**, 408–15.
- Singh, A. P. and A. D. Rey (1995) "Computer Simulation of Dynamics and Morphology of Discotic Mesophases in Extensional Flows," *Liq. Crystals*, **18**, 219–30.
- Singh, A. P. and A. D. Rey (1998) "Consistency of Predicted Shear-Induced Orientation Modes with Observed Mesophase Pitch-Based Carbon Fiber Textures," *Carbon*, **36**, 1855–9.
- Subramoney, S., J. G. Lavin, B. Fathollahi, J. L. White, and X. M. A. Bourrat (1996) "Designed Microstructures in Spinning Mesophase Pitch Fibers: Part II – Dark-Field Transmission Electron Microscopy," *Extended Abstracts, Carbon '96*, 202–3.
- Taylor, G. H. and L. F. Cross (1993) "Orthogonal Structure in Mesophase Pitch-Based Carbon Fibres," *J. Materials Sci.*, **28**, 6503–9.
- White, J. L., B., Fathollahi, and A. K. Didwania (2001) "Formation of Rippled and Zigzag Microconstituents in the Spinning of Mesophase Filaments," *Extended Abstracts, Carbon '01*.
- Yoon, S.-H., Y. Korai, and I. Mochida (1994) "Assessment and Optimization of the Stabilization Process of Mesophase Pitch Fibers by Thermal Analysis," *Carbon*, **32**, 281–7.
- Zimmer, J. E. and J. L. White (1982) "Disclination Structures in the Carbonaceous Mesophase," *Adv. in Liq. Crystals*, **5**, 157–213.